Unravelling the Effect of Strand Orientation on Exciton Migration in Conjugated Polymers

H. M. G. Correia, H. M. C. Barbosa, L. Marques and M. M. D. Ramos*

Centre of Physics and Department of Physics, University of Minho, Campus de Gualtar, 4710-057 Braga, Portugal

* Tel.: +351253604330 E-mail: marta@fisica.uminho.pt

ABSTRACT

The study of the average distance that singlet excitons travel during their lifetime in conjugated polymers has attracted considerable attention during the past decade, because of its importance in the functioning of many polymer-based optoelectronic devices, like solar cells and photodetectors. Intriguingly, different values of exciton diffusion length have been extracted from experiments on seemingly identical conjugated polymers. Here we use computer simulations to show that the observed discrepancies in the reported values of the exciton diffusion length may arise from differences in the orientation of conjugated polymer strands relative to the substrate surface, a factor which has been mostly overlooked. Our results show that, on pristine polymer nanodomains with conjugated strands perpendicular to the substrate surface, exciton migration length is approximately 30% and 40% lower than on those with parallel and random strand orientation relative to that surface, respectively, resulting from the different contents of physical traps present in nanodomains with different strand orientation. This work underlines the importance of molecular arrangement on exciton migration, and provides a

novel theoretical framework for estimating the dependence of the exciton diffusion length with the orientation of conjugated polymers strands within the nanodomains, as well as helping the design of more efficient polymer-based optical and optoelectronic devices, such as optical sensors, photodiodes, photovoltaic cells and white light-emitting diodes.

KEYWORDS: Multi-scale modelling; Exciton diffusion length; Spatial disorder; Orientation disorder; Physical trap;

1. INTRODUCTION

The migration of excitons plays a crucial role in the functioning of many optoelectronic polymeric devices, such as polymer light emitting diodes (PLEDs) and organic solar cells (OSCs) [1-3]. In what concerns OSCs, recent work [4-6] shows that by introducing a nanostructured interface between the donor (conjugated polymer) and the acceptor (low-weight organic molecule or a different conjugated polymer) materials, with a feature size of the order of the exciton diffusion length, it is possible to improve OSC efficiency significantly. This improvement is thought to result from the favourable arrangement of conjugated polymer strands, induced by geometric constraints and deposition conditions, which enhances exciton dissociation at the interface.

In an attempt to better understand the influence of strand orientation on exciton migration, several groups have measured the exciton diffusion length of the same conjugated polymers deposited using different methods [7-9]. Certain production methods are known to yield amorphous polymer films [10], whereas others produce films with complex, non-random orientations. For example, spin-coated polymer films have, on average, 15% of their conjugated segments with the long molecular axis perpendicular to

the substrate surface [11]. The remaining 85% of the segments are parallel to that surface, but show in-plane orientation disorder [12]. Their results show that the exciton diffusion length depends strongly on the conditions used to produce the film. While those observations clearly demonstrate the effect of strand orientation on exciton migration, the complexity of the arrangement of the conjugated polymer segments within the polymer film, forming nanodomains of strands with specific orientation relative to the substrate, makes it impossible to use simple arguments to understand the molecular scale origin of the different exciton diffusion lengths extracted from those experiments. In this regard, theoretical studies can be extremely helpful to unravel the underlying mechanism that is responsible for the effect of different orientation of conjugated strands on the exciton diffusion length in polymer nanodomains and their contribution to the overall exciton diffusion length of polymer films obtained from the experiments.

Earlier theoretical studies [13] did not take into account the properties of the polymer material and failed to consider the spatial arrangement of the conjugated segments within the polymer layer, a factor which later studies showed to play an important role in the physical processes underlying the functioning of polymer-based optoelectronic devices [2, 14]. More predictive theoretical methods of exciton diffusion in organic semiconductors use quantum mechanics methods to determine exciton transition rates, but consider the spatial arrangement of the conjugated segments within the polymer only very crudely by assuming an ordered lattice of exciton hopping sites. In these methods, the energy of each hopping site is modelled using a Gaussian distribution of exciton density of states inferred from experimental emission and absorption spectra of the conjugated polymer [15]. Only recently, a multi-scale approach based on time-dependent

density functional theory (TDDFT) coupled to non-adiabatic molecular dynamics simulations was used to describe the energy levels of the excitons and to calculate exciton transition rates for poly(3-hexylthiophene) (P3HT) [16]. In that work only two types of molecular arrangement – amorphous and crystalline – were considered and the effects of spatial disorder and strand orientation were taken into account in a Monte Carlo study of exciton diffusion for those specific molecular arrangements. While the use of a highly accurate parameter-free quantum mechanical method, such as TDDFT, is desirable, it becomes computationally prohibitive for large conjugated polymer systems with a realistic arrangement of the conjugated segments as in the experimental samples. Therefore, one needs to develop a less demanding computational approach, which can calculate the exciton energy levels within polymer nanodomains of reasonable size with the arrangement of conjugated segments suggested by the experiments.

In this work we propose a new and very efficient multi-scale model to elucidate the effect of strand orientation on exciton migration in nano-scale domains of conjugated polymers. This model explicitly simulates the effects of polymer nanomorphology on exciton diffusion by taking in consideration the contributions of spatial, orientation and energetic disorder within the nanodomains. These contributions result from the arrangement of conjugated polymer segments, and the dependence of exciton energy levels with the length of those segments. Our proposed model is highly computationally efficient, so simulations of entire nanodomains with molecular scale resolution are easily performed. The model's high efficiency was achieved by taking the advantage of specific characteristics of the systems being studied. Since the formation of intra-molecular excitons in the conjugated polymer segments is instantaneous when compared with the

process of exciton hopping between neighbouring conjugated segments, we can adopt a sequential multi-scale model of exciton migration in conjugated polymers. In this work we consider closely packed structures of polymer nanodomains, therefore we can neglect the time-dependent many-body interactions in these processes and use an adiabatic self-consistent quantum molecular dynamics method for calculating the exciton energy levels within the polymer nanodomains, with the arrangement of conjugated segments suggested by the experiments, and a kinetic Monte Carlo method for simulating the exciton migration in that molecular arrangement.

2. COMPUTATIONAL AND THEORETICAL METHODS

The polymers we focus in this work are poly[2-methoxy-5-(3',7'dimethyloctyloxy)-*p*-phenylene vinylene] (MDMO-PPV) and poly[2-methoxy-5-(2'ethyl-hexyloxy)-*p*-phenylene vinylene] (MEH-PPV), which are the most widely used poly(p-phenylene vinylene) (PPV) derivatives in the fabrication of polymer light emitting diodes and organic solar cells. These conjugated polymers are used in this work as model systems to address the question of the effect of strand orientation on exciton migration that applies to other conjugated backbone polymers explored in the scientific community at present. Conjugated polymer chains typically have kinks and twists which interrupt conjugation. Polymer chains can thus be considered as arrays of conjugated segments of varying length, each segment behaving as a separate photon absorption and emitting centre [17]. Pristine polymer films consist of an arrangement of nanodomains, where in each nanodomain the ensemble of conjugated polymer segments have a preferential orientation. Our simulations focus on the single-nanodomain scale: we create models of

single nanodomains where the orientation of each conjugated segment is explicitly represented. We use these models to investigate how changes in the average orientation of polymer segments affect exciton migration. The polymer nanodomains used for our simulations have 100 nm height (the typical thickness of polymer-based films in optoelectronic devices) and 20 nm width (dimensions much larger than the exciton migration length in conjugated polymers with spatial disorder), consisting of 3D-networks of conjugated polymer segments randomly distributed in space. The polymer nanodomains were built considering that all segments have their long molecular axis parallel, perpendicular and randomly oriented relative to the substrate surface (see figure 1) and a Gaussian distribution of segment lengths with a mean value of 7 monomers (see figure 3 (a)) in agreement with the average conjugation length predicted for PPV derivatives [18]. In the case of conjugated segments with their long molecular axis oriented parallel to substrate surface, we considered a random orientation of those axes in the planes parallel to the substrate surface, as illustrated in Figure 1, middle panels. To better sample the influence of orientation on exciton migration, 30 realizations of each type of polymer network (parallel, perpendicular and random) are created. For each PPV derivative, simulations are performed for every realization of the polymer network. With this approach we can thus investigate the effect of spatial and orientation disorder and of molecular identity on exciton migration.

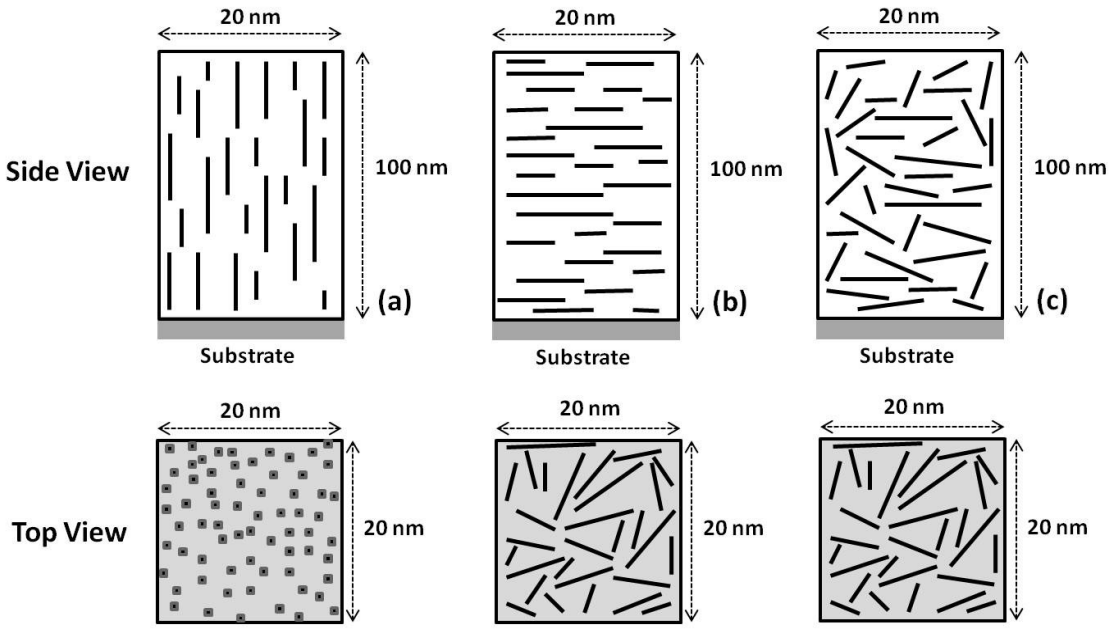

Figure 1. Schematic diagram of the projection of the long molecular axis of the conjugated segments within the polymer nanodomains on the direction parallel (side view) and perpendicular (top view) to the substrate surface (shadow area) for perpendicular (a) parallel (b) and random (c) orientation of the segments axis relative to the substrate surface.

When a photon is absorbed in the ensemble of conjugated polymers segments, which work like chromophores, there is an optical excitation on a single conjugated segment leading to the formation of a singlet exciton on that polymer segment. Since there is a very strong level of electron-lattice coupling in conjugated polymer segments, it is necessary to perform self-consistent calculations of electronic wave functions and atomic positions in order to properly study exciton formation in polymer strands. We use the self-consistent quantum molecular dynamics method, implemented in the CHEMOS code [19, 20], to calculate the energy and the atomic charge distribution of the relaxed

uncharged conjugated polymer segments with different conjugation lengths in the lowest singlet excited state with the lengths present in the polymer networks. The method used in this work solves simultaneously, for each conjugated segment, the Schrödinger equation, using the semi-empirical molecular orbital theory which works at the CNDO (Complete Neglect of Differential Overlap) level within a minimum basis set [21, 22] for obtaining its electronic structure, and Newton's equations, for obtaining the nuclear motion, using the forces calculated self-consistently at each time step, assuming that the initial velocities of all nuclei are zero. Although nuclear motion and the effect of intrinsic fluctuations, resulting from self-consistent inter-atomic interactions, are included in the quantum molecular dynamics simulations performed in this work, no rescaling of nuclear velocities was done during the simulations in order to assure quantum molecular dynamics simulations at room temperature. Calculations of electronic structure and atomic relaxation where performed in parallel until a minimum energy is achieved for each polymer strand.

Using this strategy it was possible to obtain the electron-hole distance (R_0) that results of singlet exciton formation in the polymer strands, as well as the energy barrier height that the exciton has to overcome to hop between two strands, which are used as atomistic parameters in our mesoscopic model. The lowest singlet excited state was obtained by promoting an electron from the highest occupied molecular orbital (HOMO) to the lowest unoccupied molecular orbital (LUMO) of the ground state of isolated PPV derivatives segments considered in this work. The exciton formation induces changes in Mulliken atomic charges of the atoms of the polymer backbone similar to a dipole (see

Figure 2) with an average distance R_0 between the positive and negative charge distribution.

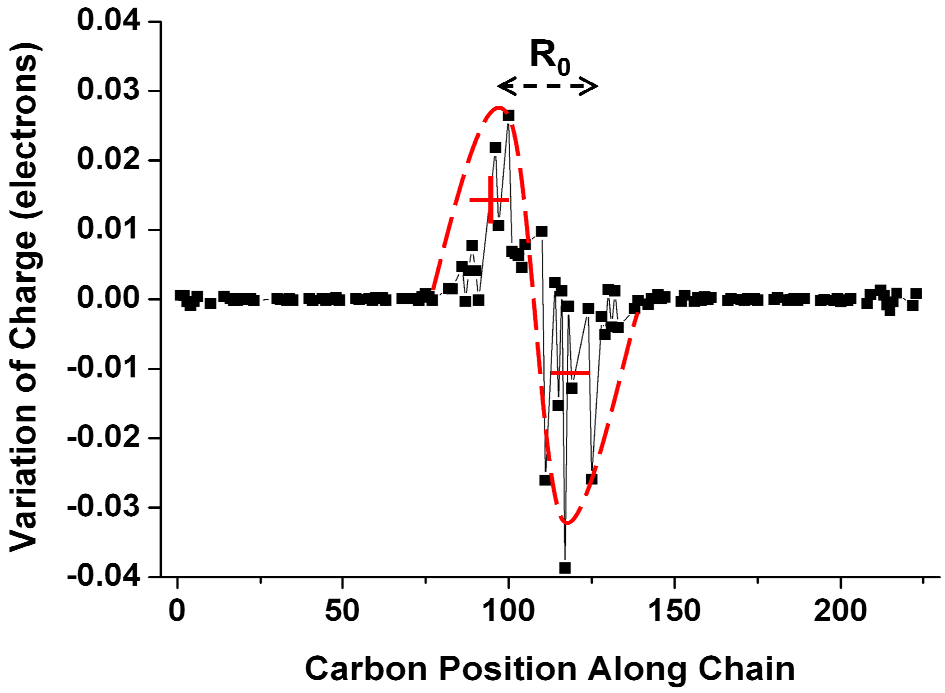

Figure 2. Changes in Mulliken atomic charges in carbon atoms relative the ground state values of a PPV derivative strand with 16 repeat units induced by singlet exciton formation. R_0 represents the average distance between positive and negative charge distribution in the polymer strand atoms.

When an exciton hops between two neighbour polymers strands, an electron returns to the HOMO in the donor polymer strand and simultaneously an electron is promoted to the LUMO in the acceptor. The energy barrier height for this exciton hopping can thus be calculated by:

$$\Delta E_{ij} = (E_j^* + E_i) - (E_i^* + E_j) \qquad (1)$$

being $E^*_{i(j)}$ and $E_{i(j)}$ the energy of the conjugated polymer segments of the donor (acceptor) in the excited and ground state, respectively. Considering as reference the energy of excited and ground state of polymer strands with 7 monomers length, the energy barrier established for exciton hopping between a polymer strands with this length with others with different lengths (figure 3(b)) is a good approximation of the exciton energetic disorder present in closely packed structures within the polymer nanodomains.

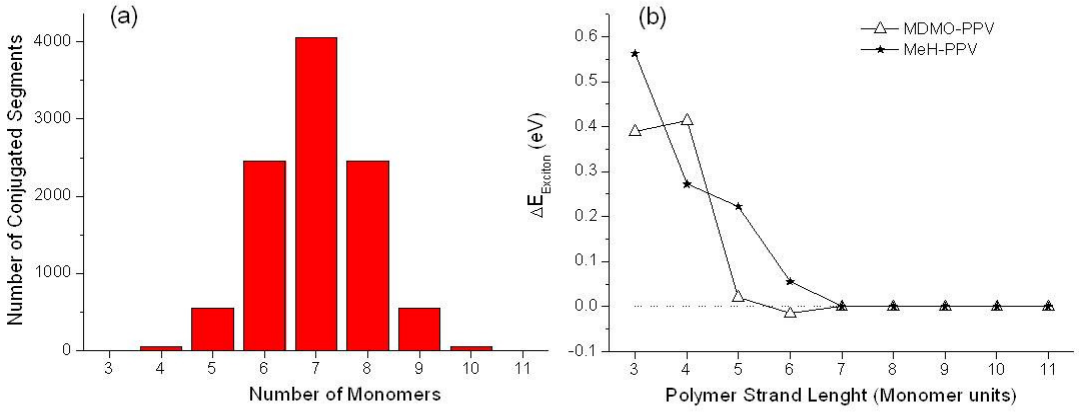

Figure 3. Distribution of the conjugated segment lengths within polymer networks with a volume of 40000 nm^3 (a) and the energy barrier height that a singlet exciton has to overcome to hop from a conjugated segment of 7 monomers length to a segment with different length, shown in the horizontal-axis of the plot, for the PPV derivatives considered in this work (b).

Our previous publication [23] shows that this self-consistent approach based on the CNDO method correctly predicts the right trends for the molecular properties of PPV and yields exciton migration parameters in very good agreement with experiment. Since PPV and its derivatives have the same conjugated backbone, we expect the predicted trends for

the exciton energetic disorder in PPV derivatives due to their different molecular properties to be also reliable.

To simulate the singlet exciton migration in the built polymer networks, a uniform randomly distributed pulse of 100 excitons is created inside those networks. This size of the excitation pulse was selected to provide meaningful statistics and averages while still keeping the photon density small enough to avoid exciton-exciton annihilation [24]. A spatially random distribution of excitons was chosen because our atomistic calculations have shown that the probability of photon absorption does not depend on the length of the conjugated segments [25]. Each exciton created on a conjugated segment has an intrinsic lifetime given by:

$$t_i = -\frac{\ln(X)}{w_0} \qquad (2)$$

where X is a random number between 0 and 1, and w_0 represents the decay probability of the excited state per unit time by spontaneous photon emission (radiative decay rate), which is assumed to have a value of 10^9 s^{-1}, in agreement with the radiative decay rate of PPV derivatives [26] measured experimentally.

Our atomistic calculations show that the formation of a singlet exciton on a conjugated polymer segment, due to light absorption, occurs in the central region of that segment leading to a dipole charge distribution along the conjugated polymer backbone [27], which corresponds to a Frenkel-type exciton. These results suggest that excitons tend to migrate between the centres of neighbouring conjugated segments by a thermally activated hopping process mediated by a dipole-dipole interaction. On the other hand, the fact that a dipole is formed along the segment axis and the orientation of the polymer

segments relative to each other is not isotropic along the polymer film, which can affect exciton dynamics, must be taken into account in the model to simulate singlet exciton migration within the polymer nanodomains. In our model the exciton hopping rate is given by:

$$w_{ij} = w_{0,dip-dip} \times \begin{cases} 1 & for \quad r_{ij} < R \\ \left(\frac{R}{r_{ij}}\right)^6 & for \quad r_{ij} \geq R \end{cases} \times \begin{cases} 1 & for \quad \Delta E_{ij} \leq 0 \\ \exp\left(-\frac{\Delta E_{ij}}{kT}\right) & for \quad \Delta E_{ij} > 0 \end{cases} \qquad (3)$$

where $w_{0,dip-dip}$ is assumed to have the value of 3.3×10^{11} s^{-1} [28] for inter-segment hopping of the same polymer chain or different chains. The critical distance *R*, above which the hopping frequency is dependent on the distance between the centre of polymer strands according to the mechanism of dipole-dipole interaction, is given by $R^6 = R_0^6 \times \left[\cos(\theta_{ij}) - 3\cos(\theta_i)\cos(\theta_j)\right]^2$, where R_0=*1.3nm* is the electron-hole distance in the singlet exciton formed in the PPV backbone and is obtained from the self-consistent quantum molecular dynamics calculations, θ_{ij} is the angle between the dipole directions in strands *i* and *j* involved in the hopping process and $\theta_{i(j)}$ is the angle between the dipole direction of strand *i(j)* and the hopping direction, ΔE_{ij} is the energy barrier for exciton hopping, *k* is the Boltzmann constant and *T* is the temperature, which is assumed to have a value of 300K in this work. Here $f = \left[\cos(\theta_{ij}) - 3\cos(\theta_i)\cos(\theta_j)\right]$ is a factor resulting from the orientation of transition dipoles in the polymer network [29], and reflects the correlated orientation disorder of the conjugated segments within the polymer nanodomain.

Since the exciton relaxation time within each conjugated segment is much lower than the hopping time, we assume that exciton relaxation takes place before each hopping event occurs. For each exciton the only hopping process that takes place is the one with the greatest hopping frequency. After each hopping event, there is a waiting time given by:

$$\tau = -\frac{\ln(X)}{w_{ij}} \tag{4}$$

X being a random number uniformly distributed between 0 and 1.

On the first computer iteration it is established a queue of events with increasing time. The event with the smallest waiting time takes place and it is removed from the queue. This waiting time is then subtracted from the remaining time of the other events and a new hopping event is inserted in the queue. The hopping event associated with an exciton is removed from the queue when its lifetime is over. Using this strategy [30], we follow the time evolution of exciton migration within the polymer network and calculate the maximum distance that each exciton reaches from its formation position, which corresponds to the migration length of that exciton. The average distance that excitons migrate during their lifetime, usually called the exciton diffusion length, can then be determined by:

$$\langle L_D \rangle = \frac{\sum_{i=1,N} L_i}{N} \tag{5}$$

where N is the number of excitons created in the polymer network and L_i being the migration length of each one of them. The calculated exciton diffusion length for each PPV derivative is averaged over 30 different computer simulations, each one corresponding to a different polymer network in order to avoid artefacts of the calculations caused by any structural defect created during the building of the polymer

network. We note that the 30 polymer networks used for simulating exciton migration for each average strand orientation are the same for both PPV derivatives, and consequently the results obtained for each strand orientation have the same spatial and orientation disorders but only differ on the energetic disorder as a result of the different molecular properties of both polymers.

3. RESULTS AND DISCUSSION

In figure 4 we show the results obtained for the distribution of the created excitons within the polymer network per conjugated segment length and their decay positions, for the PPV derivatives with conjugated segments with their long axis parallel to the substrate surface. Perpendicular and random orientations of the segments axis relative to the substrate surface show similar behaviour (not shown). The analyses of these results show interesting features. One is that the excitons formed in the polymer network migrate from short conjugated segments (higher energy sites) towards longer conjugated segments (lower energy sites), which is in agreement with experimental observations [31, 32] and recent theoretical simulations [16]. This downhill migration is due to the strand length distribution inside the polymer networks. Another important aspect is that the maximum number of exciton decays occurs in conjugated segments with the same length for the two PPV derivatives and that number does not depend significantly on the polymer strand orientation (perpendicular and random orientation not shown). Our results also show that the migration of excitons from higher energy states to lower energy states is followed by thermally activated migration to hopping sites with similar energy, in agreement with previous theoretical works [16].

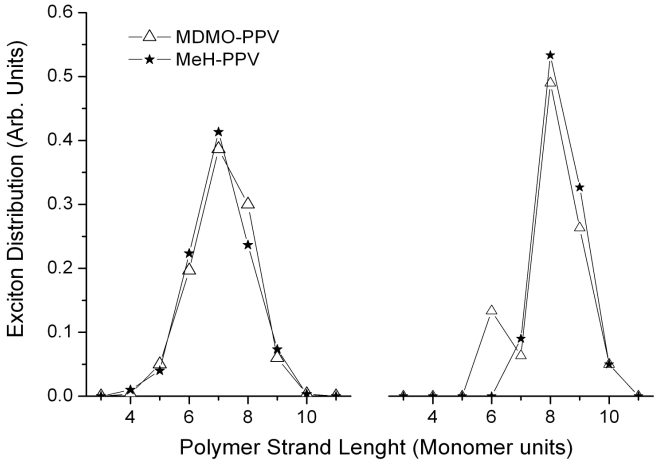

Figure 4. Fraction of excitons created (left-hand side) and the corresponding exciton decay events (right-hand side) within the polymer network for the PPV derivatives considered in this work, with conjugated segments with their long axis parallel to the substrate surface. The marks indicate the data points that were calculated explicitly, whilst the curves are simply a guide to the eye.

Table 1 summarizes the calculated exciton diffusion lengths of MDMO-PPV and MEH-PPV for polymer networks with conjugated segments with their long axis oriented parallel and perpendicular relative to the substrate surface and randomly oriented, extracted directly from the simulations with no fitting parameters. These results show that the orientation of polymer strands relative to the substrate surface has a dramatic effect on the average distance that excitons migrate during their lifetime, for all conjugated segment orientations considered in this work. In contrast, the exciton energetic disorder, which results from the molecular scale polymer properties, has a much less pronounced effect.

Table 1. Calculated exciton diffusion length in PPV derivatives (nm) for different orientations of the long-axis of conjugated segments relative to the substrate surface.

Conjugated segment orientation.	MDMO-PPV	MEH-PPV
Perpendicular	3.360	3.870
Parallel	4.727	5.546
Random	5.630	6.310

In order to assess the validity of our model to predict the exciton diffusion length in nanodomains with different average orientation of the conjugated segments relative to the substrate surface, we use the results obtained from the simulations for MDMO-PPV shown in Table 1 and calculate the exciton diffusion length for spin-coated films L_D = (0.15×3.360+0.85×4.727) nm = 4.522 nm, using the percentages of conjugated segments with the molecular axis oriented parallel and perpendicular to the substrate film surface taken from experiments [11]. We found that the predicted result for the exciton diffusion length of the spin-coated MDMO-PPV film, is in excellent agreement with the experimental finding (4.5 nm) [32], which suggests that the proposed model, which includes correlated orientation disorder, is able to predict correctly the effect of conjugated segment orientation on nanodomains within the polymer films with spatial disorder. The results obtained with our methodology, for the random orientation, are in the same order of magnitude as those predicted by the first-principles simulations for another conjugated polymer [16], but they were obtained with much less computational effort.

According to our results, the polymer nanodomains with conjugated segments perpendicular to the substrate surface have the lowest exciton diffusion length, its value being approximately 30% lower than on nanodomains with strand orientation parallel to that surface and approximately 40% lower than on nanodomains with random strand orientation. Note also that, this evolution of exciton diffusion length with segment orientation relative to the substrate surface is similar for both PPV derivatives considered in this work, which indicates that this result is related with the percolation characteristics of the three different types of arrangement of conjugated strand.

In fact, we found that in polymer networks with all conjugated segments oriented perpendicular to the substrate surface there is a significant number of excitons unable to travel away from their creation position, being imprisoned in structural dead ends (physical traps) until they decay (see Table 2). This type of physical traps behave in a similar way to morphological defects already highlighted in the experiments as a result of polymer chain stacking faults in pristine polymer films [33, 34]. The number of physical traps decreases when strands are on average parallel to the substrate surface, but reaches its minimum value for a random strand orientation. The dead ends (physical traps) arise from the distribution of hopping sites (and lengths of polymer segments holding them) in the neighbourhood of a strand before the first hopping event occurs. When the new hopping sites are far away from the created exciton, the first hopping event never occurs during its lifetime, even if that hopping event is energetically favourable, and the exciton is physically trapped. If the new hopping sites are close to the exciton position after the first hopping event takes place, the occurrence of a second hopping event to a new conjugated segment (see the percolation path in Figure 5) is limited by the availability of

energetically favourable hopping sites that depends on the length of the conjugated segment that holds the new hopping site. However, the percolation path never takes place if the hopping distance for the second hopping event to a new conjugated segment is much larger than a certain value even if that hopping event is energetically favourable. Under certain conditions the exciton can hop back to its creation position, being trapped between the two neighbouring conjugated strands, which correspond to a migration length equal to the first hopping distance.

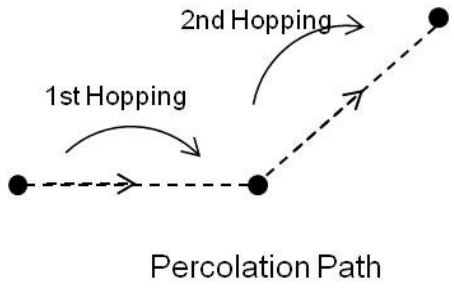

Figure 5. Schematic diagram of a percolation path for an exciton between two consecutive hopping events.

The dead ends act as physical traps in spatially disordered polymer networks, which limit the exciton diffusion length in pristine conjugated polymers in a similar way to chemical traps in a well-ordered network of exciton hopping sites [15], corresponding to a crystalline polymer structure with chemical impurities. From table 2 we can also find that the number of physically trapped excitons in pristine polymer networks with spatial disorder decreases strongly with the increase of orientation disorder, the effect being more pronounced for MDMO-PPV.

Table 2. The effect of conjugated segment orientation relative to the substrate surface on the percentage of physically trapped excitons in PPV derivatives.

Conjugated segment orientation	MDMO-PPV	MEH-PPV
Perpendicular	13.77	7.53
Parallel	9.70	4.43
Random	7.27	3.57

In order to assess the effect of strand orientation relative to the substrate surface on the ability of the excitons to percolate within the polymer network and reach the maximum diffusion length, we calculate the maximum difference in the length of two consecutive hopping events along the percolation path. The values obtained for polymer nanodomains with perpendicular, parallel and random orientation of their conjugated segments relative to the substrate surface are 0.6 nm, 0.4 nm and 0.3 nm, respectively. These results show that the increase of orientation disorder in polymer networks with spatial disorder (non-crystalline networks) decreases the maximum distance between consecutive hops, which favours the percolation of excitons within the polymer networks, and consequently favours the increase of exciton diffusion length.

The novel multi-scale model that we developed allows us to unravel the influence of polymer strand orientation on exciton diffusion length in a realistic polymer layer, with modest computational resources. It also allows us to predict the molecular scale origin of the effect of polymer nanomorphology on exciton diffusion length, a link which has not been established so far.

4. CONCLUSIONS

Through a novel multi-scale modelling approach it was possible to provide insight into the mechanisms that govern the exciton migration process in pristine conjugated polymers and unravel the effect of molecular properties and molecular arrangement on exciton dynamics. Our results show that the orientation of conjugated segments of PPV derivatives significantly affects their exciton diffusion. Using the single-nanodomain exciton diffusion lengths calculated from our simulations and the experimentally determined fraction of different types of domains for spin-coated films of PPV derivatives, and without any fitting parameters, we calculated the average exciton diffusion length for MDMO-PPV. Our calculated exciton diffusion length is in excellent agreement with the experimental one, establishing, in this way, a cause-effect between the orientation of the conjugated polymer segments relative to the substrate surface and the exciton diffusion length within the polymer nanodomain. Most important, we found a correlation between orientation disorder, the amount of physically trapped excitons and the ability for exciton percolation, meaning that suppressing orientation disorder in pristine non-crystalline conjugated polymers increases the physical trapping of excitons, decreases their percolation ability and, consequently, decreases their diffusion length. This work shows the valuable contribution of a novel multi-scale theoretical framework for providing not only for a physical interpretation of experimental data but also information about exciton dynamics in conjugated polymer systems which is hard to obtain directly from the experiments, with much less computational effort than the first-principles multi-scale methods. The results from this work put in evidence the importance of molecular arrangement on exciton diffusion length in conjugated polymers, which

must be taken in consideration in the optimization of polymer-based optical and optoelectronic devices.

ACKNOWLEDGEMENTS

We would like to express our gratitude to Professor Marshall Stoneham for inspiring this work and for the past useful discussions on the subject. This work was supported by FEDER through the COMPETE Program and by the Portuguese Foundation for Science and Technology (FCT) in the framework of the Strategic Project PEST-C/FIS/UI607/2011, and under the projects CONC-REEQ/443/EEI/2005 and PEst-C-FIS/UI607/2011-2012. Two of us (H.M.G.C. and H. M. C. B.) are also indebted to FCT and POPH for financial support the post-doctoral grants SFRH/BPD/64554/2009 and SFRH/BPD/80561/2011.

REFERENCES

[1] G. Li, R. Zhu, Y. Yang, Nat. Photonics, 6 (2012) 153-161.

[2] A. Moliton, J.M. Nunzi, Polym. Int., 55 (2006) 583-600.

[3] P. Peumans, A. Yakimov, S.R. Forrest, J. Appl. Phys., 93 (2003) 3693-3723.

[4] X. He, F. Gao, G. Tu, D. Hasko, S. Huettner, U. Steiner, N.C. Greenham, R.H. Friend, W.T.S. Huck, Nano Lett., 10 (2010) 1302-1307.

[5] F. Liu, Y. Gu, J.W. Jung, W.H. Jo, T.P. Russell, J. Polym. Sci., Part B: Polym. Phys., 50 (2012) 1018-1044.

[6] Y. Yang, K. Mielczarek, M. Aryal, A. Zakhidov, W. Hu, Acs Nano, 6 (2012) 2877-2892.

[7] M.M. Alam, S.A. Jenekhe, Chem. Mater., 16 (2004) 4647-4656.

[8] A.J. Lewis, A. Ruseckas, O.P.M. Gaudin, G.R. Webster, P.L. Burn, I.D.W. Samuel, Org. Electron., 7 (2006) 452-456.

[9] D.E. Markov, C. Tanase, P.W.M. Blom, J. Wildeman, Phys. Rev. B, 72 (2005) 045217.

[10] K. Koynov, A. Bahtiar, T. Ahn, R.M. Cordeiro, H.H. Horhold, C. Bubeck, Macromolecules, 39 (2006) 8692-8698.

[11] H. Becker, S.E. Burns, R.H. Friend, Phys. Rev. B, 56 (1997) 1893-1905.

[12] T.G. Backlund, H.G.O. Sandberg, R. Osterbacka, H. Stubb, M. Torkkeli, R. Serimaa, Adv. Funct. Mater., 15 (2005) 1095-1099.

[13] P.K. Watkins, A.B. Walker, G.L.B. Verschoor, Nano Lett., 5 (2005) 1814-1818.

[14] M. Jaiswal, R. Menon, Polym. Int., 55 (2006) 1371-1384.

[15] S. Athanasopoulos, E. Hennebicq, D. Beljonne, A.B. Walker, J. Phys. Chem. C, 112 (2008) 11532-11538.

[16] X. Zhang, Z. Li, G. Lu, Phys. Rev. B, 84 (2011) 2352081-2352088.

[17] D.E. Markov, P.W.M. Blom, Phys. Rev. B, 74 (2006) 0852061-0852065.

[18] B.G. Sumpter, P. Kumar, A. Mehta, M.D. Barnes, W.A. Shelton, R.J. Harrison, J. Phys. Chem. B, 109 (2005) 7671-7685.

[19] D.S. Wallace, in: D. Phil. Thesis, University of Oxford, 1989.

[20] D.S. Wallace, A.M. Stoneham, W. Hayes, A.J. Fisher, A.H. Harker, J. Phys. Condens. Matter, 3 (1991) 3879-3903.

[21] J.N. Murrell, A.J. Harget, Semi-empirical self-consistent-field molecular orbital theory of molecules, Wiley-Interscience,, London, 1972.

[22] J.A. Pople, D.L. Beveridge, Approximate Molecular Orbital Theory, McGraw-Hill, New York, 1970.

[23] H.M.C. Barbosa, H.M.G. Correia, M.M.D. Ramos, J. Nanosci. Nanotechnol., 10 (2010) 1148-1152.

[24] I.G. Scheblykin, A. Yartsev, T. Pullerits, V. Gulbinas, V. Sundstrom, J. Phys. Chem. B, 111 (2007) 6303-6321.

[25] H.M.G. Correia, in: PhD Thesis, University of Minho, Braga, 2007.

[26] U. Lemmer, R.F. Mahrt, Y. Wada, A. Greiner, H. Bassler, E.O. Gobel, Appl. Phys. Lett., 62 (1993) 2827-2829.

[27] M.M.D. Ramos, H.M.G. Correia, Appl. Surf. Sci., 248 (2005) 450-454.

[28] M. Scheidler, U. Lemmer, R. Kersting, S. Karg, W. Riess, B. Cleve, R.F. Mahrt, H. Kurz, H. Bassler, E.O. Gobel, P. Thomas, Phys. Rev. B, 54 (1996) 5536-5544.

[29] T.S. Ahn, N. Wright, C.J. Bardeen, Chem. Phys. Lett., 446 (2007) 43-48.

[30] J.J. Lukkien, J.P.L. Segers, P.A.J. Hilbers, R.J. Gelten, A.P.J. Jansen, Phys. Rev. E, 58 (1998) 2598-2610.

[31] R. Kersting, U. Lemmer, R.F. Mahrt, K. Leo, H. Kurz, H. Bassler, E.O. Gobel, Phys. Rev. Lett., 70 (1993) 3820-3823.

[32] O.V. Mikhnenko, F. Cordella, A.B. Sieval, J.C. Hummelen, P.W.M. Blom, M.A. Loi, J. Phys. Chem. B, 112 (2008) 11601-11604.

[33] B.A. Gregg, J. Phys. Chem. C, 113 (2009) 5899-5901.

[34] B.A. Gregg, Soft Matter, 5 (2009) 2985-2989.